XXI Seminarium

ZASTOSOWANIE KOMPUTERÓW W NAUCE I TECHNICE' 2011
Oddział Gdański PTETiS
Referat nr 28

REPRESENTATION OF MAGNETIC HYSTERESIS IN TAPE WOUND CORE USING PREISACH'S THEORY

Andrzej WILK

Politechnika Gdańska, ul. G. Narutowicza 11/12, 80-952 Gdańsk,
tel: 058 347 1087 fax: 058 341 0880 e-mail: awilk@ely.pg.gda.pl

Abstract: This paper presents a mathematical model for the hysteresis phenomenon in ferromagnetic tape wound core. The classical scalar Preisach model of hysteresis is used to simulate magnetic behavior of the grain oriented silicon strip of ET114-27 type. Determination of *B*-*H* hysteretic curve is based on measurement of the downward and upward trajectories of the limiting loop. The Everett function and the Preisach distribution function of ET114 material are presented. The model has been validated by comparing measured and calculated results obtained from tests. Experiments and simulations confirm the accuracy of worked out model.

Keywords: Magnetic hysteresis, scalar Preisach model, Everett function, Preisach distribution function.

1. INTRODUCTION

In all ferromagnetic material there is nonlinear relation between magnetic flux density *B* and magnetic field intensity *H* defined as magnetization curve *B*(*H*). This type of curve is always a hysteresis curve. When a ferromagnetic substance is under the influence of a time dependent field intensity there is a lag between *B* and *H*. The material passes through the loop of hysteresis curve and the shape of this loop depends on the type of material used in magnetic core and range of exciting field intensity. The hysteretic *B*(*H*) curve is very important in certain phenomena associated with power systems, such as the inrush of magnetizing current, ferro-resonance, and residual flux in transformer cores [1-3]. Ferroresonant state can produce much large currents and voltages than normal and hysteresis can noticeable influence on switching currents and voltages. A cyclic variation of magnetic flux generates also dissipation of an amount of energy proportional to the area of hysteresis loop. This is in most cases detrimental to the operation of the device due to heating of the material.

Several efforts to model magnetic hysteresis have been until now reported. Among many models proposed so far, the model based on the Preisach's theory [4] seems to be a good method for accurate modeling and prediction of the magnetic characteristic. The Preisach model (PM) had been initially utilized in the area of magnetics but its mathematical generality suggested implementation of this model in many areas of science. A pure mathematical form of the PM separated from its physical meaning was proposed by Krasnosel'skii [5]. This approach was further developed by Mayergoyz [6-8] for determining the conditions for the representations of the hysteresis nonlinearities and generalization of the PM. Nowadays there are several generalizations of the original PM (generalized PM, moving PM, dynamic PM, vector PM) in other to improve its ability to represent complex experimental results. These modifications of PM are characterized and summarized in [9].

In this paper, only scalar Preisach model is introduced for representation of magnetic hysteresis in tape wound core. The numerical aspects and implementation of used model are thoroughly discussed. The Preisach distribution and the Everett functions are derived in analytical form. Parameter identification procedure requires only the limiting ascending and descending *B*-*H* curves. The results predicted by the model have been successfully verified by experiments.

2. THE SCALAR PREISACH MODEL

2.1. Summary of Preisach's theory

In the classical Preisach model a ferromagnetic material is made up of infinite set of magnetic dipoles, each having magnetic characteristics with two separate, randomly distributed properties α, β as shown in Fig.1.

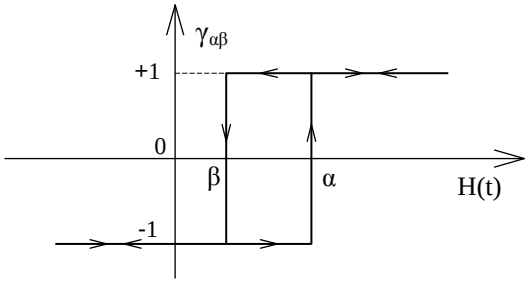

Fig.1. Rectangular hysteresis loop of elementary dipole

Each dipole has rectangular hysteresis loop and is defined as mathematical operator $\gamma_{\alpha\beta}(H)$ that can assume only two values, +1 (positively switched) and -1 (negatively

Recenzent: Prof. dr hab. inż. Kazimierz Jakubiuk – Wydział Elektrotechniki i Automatyki Politechnika Gdańska

switched). The relationship between magnetic field intensity $H(t)$ and flux density $B(t)$ is expressed in the integral form as

$$B(t) = \iint_{\alpha \geq \beta} \mu(\alpha,\beta)\gamma_{\alpha\beta}(H(t))d\alpha d\beta \qquad (1)$$

where $\mu(\alpha,\beta)$ is a finite weight function having nonzero values within the limits of major hysteresis loop. The term $\mu(\alpha,\beta)$ is also called the Preisach distribution function and can be regarded as a material constant.

The equation (1) can be geometrically interpreted on the Preisach diagram as shown in Fig.2. On this diagram an isosceles right-angled triangle indicates range of coordinates $-H_s \leq \beta \leq \alpha \leq H_s$ where weight function $\mu(\alpha,\beta)$ is nonzero and where H_s is the saturation magnetic field intensity.

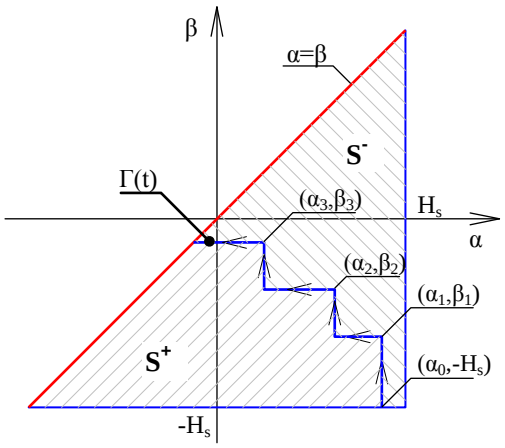

Fig.2. A geometric interpretation of the hysteresis model on Preisach diagram: S^+ – region positively switched dipoles, S^- – region negatively switched dipoles

Axis α corresponds to increments of field intensity H whereas axis β to decrements of H. At each instant of time t the α-β plane is divided into two areas $S^+(t)$ and $S^-(t)$ by the boundary line $\Gamma(t)$. Coordinates (α,β) in $S^+(t)$ area correspond to an operator $\gamma_{\alpha\beta}(H)=1$, and coordinates in $S^-(t)$ area correspond to an operator $\gamma_{\alpha\beta}(H)=-1$. Taking into account the geometrical interpretation, the equation (1) can be equivalently expressed as

$$B(t) = \iint_{S^+(t)} \mu(\alpha,\beta)d\alpha d\beta - \iint_{S^-(t)} \mu(\alpha,\beta)d\alpha d\beta \qquad (2)$$

The interface $\Gamma(t)$ between S+ and S- results from local maxima and minima of H at previous states $\{(\alpha_0,-H_s);(\alpha_1,\beta_1);(\alpha_2,\beta_2);(\alpha_3,\beta_3)\}$ (see Fig.2) and the present state of magnetization. The interface $\Gamma(t)$ is usually a staircase line attached to the $\alpha=\beta$ line and moves along the $\alpha=\beta$ line when the $H(t)$ changes.

2.2. The states of magnetization and the corresponding Preisach's diagrams

For an unmagnetised material there are as many dipoles in the $\gamma_{\alpha\beta}(H)=1$ state as in the $\gamma_{\alpha\beta}(H)=-1$ state. This also means that there are as many dipoles in the region S^+ as there are in the region S^- and formula (2) performs condition

$$B = \iint_{S^+} \mu(\alpha,\beta)d\alpha d\beta - \iint_{S^-} \mu(\alpha,\beta)d\alpha d\beta = 0 \qquad (3)$$

The corresponding interface $\Gamma(t)$ at $H=0$ and $B=0$ on the Preisach diagram is shown in Fig.3.

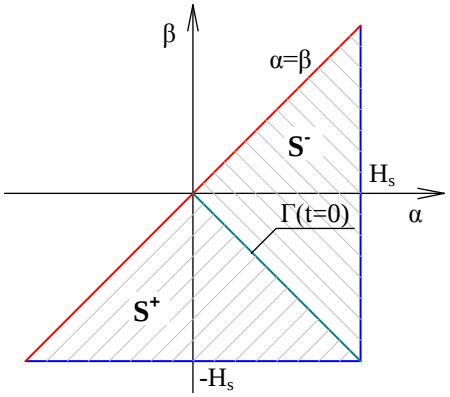

Fig.3. Preisach diagram for an unmagnetised material

A typical magnetic characteristic which consist of initial curve, limiting downward, and limiting upward curves is shown in Fig.4. When a positive magnetic field is now applied to the material, then those negative dipoles satisfying the condition $\alpha<H$ will change state. B-H curve follows from P0 to P1 point and next to P2 on the initial magnetization curve. The corresponding interface $\Gamma(t)$ on the Preisach diagram for P1 point is shown in Fig.5.

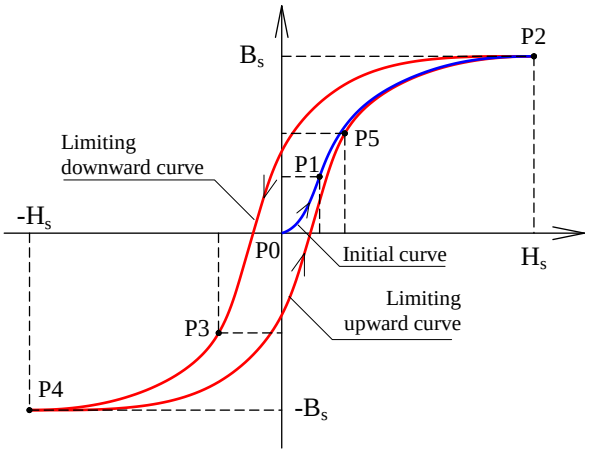

Fig.4. A typical $B(H)$ characteristic for a major loop

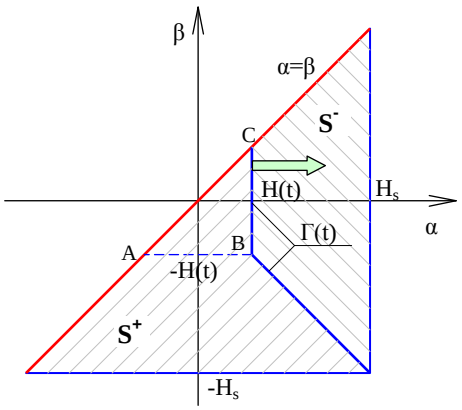

Fig.5. Preisach diagram for the initial magnetization curve

From the Preisach diagram shown in Fig.5 the flux density B_i given by initial curve (subscript i) can be expressed as

$$B_i(H) = \iint_{S^+} \mu(\alpha,\beta)d\alpha d\beta - \iint_{S^-} \mu(\alpha,\beta)d\alpha d\beta$$
$$= \iint_{region ABC} \mu(\alpha,\beta)d\alpha d\beta = T(H,-H) \quad (4)$$

where *region ABC* is the triangular area of integration. The term $T(\alpha,\beta)$ is called the Everett function [10] and is the integral of the Preisach function over the right-angled triangle formed by the line $\alpha=\beta$ and vertex (α,β); therefore

$$T(\alpha,\beta) = \int_{\beta}^{\alpha}\int_{\beta}^{\alpha'} \mu(\alpha',\beta')d\beta' d\alpha' = \int_{\beta}^{\alpha}\int_{\beta'}^{\alpha} \mu(\alpha',\beta')d\alpha' d\beta' \quad (5)$$

In equation (5) the primes are used to denote the variables involved in the integration. The unprimed variables are the limits of the integral. If the applied field $H>H_s$, the material is magnetically saturated to positive state and magnetic flux density is single-valued function of H.

When the applied field is now reduced, then, because of the hysteresis property of each dipole, those positive dipoles that satisfy the condition $H<\beta$ will change state. The *B-H* curve follows from P2 point to P3 point and next to P4 on the descending trajectory of the limiting loop. The corresponding interface $\Gamma(t)$ on the Preisach diagram for P3 point is shown in Fig.6.

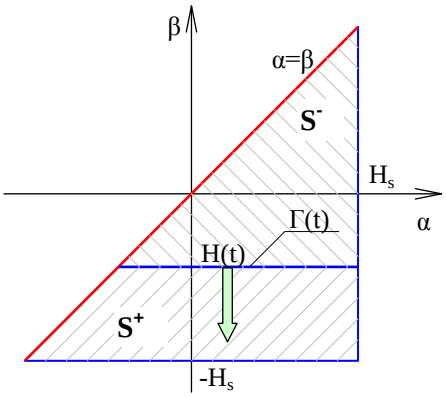

Fig.6. Preisach diagram on the limiting downward trajectory

From the corresponding Preisach diagram (Fig.6) the flux density B_d given by limiting downward trajectory (subscript *d*) can be expressed as

$$B_d(H) = \iint_{S^+} \mu(\alpha,\beta)d\alpha d\beta - \iint_{S^-} \mu(\alpha,\beta)d\alpha d\beta$$
$$= B_i(H_s) - 2T(H_s,H) \quad (6)$$

If the applied field $H<-H_s$, the material is magnetically saturated to negative state and magnetic flux density is single-valued function of H.

When the applied field is subsequently increased, then, those negative dipoles that satisfy the condition $H>\alpha$ will change state. The *B-H* curve follows from P4 point to P5 point on the ascending trajectory of the limiting loop. The corresponding interface $\Gamma(t)$ on the Preisach diagram for P5 point is shown in Fig.7. From the corresponding Preisach diagram (Fig.7) the flux density B_u given by limiting upward trajectory (subscript *u*) can be expressed as

$$B_u(H) = \iint_{S^+} \mu(\alpha,\beta)d\alpha d\beta - \iint_{S^-} \mu(\alpha,\beta)d\alpha d\beta$$
$$= B_i(-H_s) + 2T(H,-H_s) \quad (7)$$

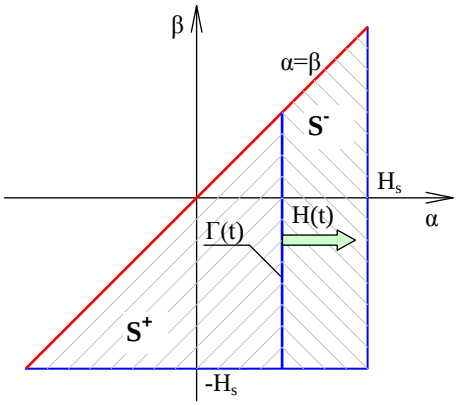

Fig.7. Preisach diagram on the limiting upward trajectory

2.3. General trajectories from reversal points

In general, every upward trajectory and every downward trajectory has local maximum and local minimum in reversal points. The flux density induced from the *n*th (last) reversal (maximum) point on the downward trajectory can be given by

$$B(H) = B(H_n) - 2T(H_n,H) \quad (8)$$

Similarly, the flux density induced from the *n*th (last) reversal (minimum) point on the upward trajectory can be calculated as

$$B(H) = B(H_n) + 2T(H,H_n) \quad (9)$$

The downward and upward trajectories can be involved to calculate $T(\alpha,\beta)$ by means of the following formula [11]

$$T(\alpha,\beta) = \frac{B_u(\alpha) - B_d(\beta)}{2} + \int_{-H_s}^{\beta}\int_{\alpha}^{H_s} \mu(\alpha',\beta')d\alpha' d\beta' \quad (10)$$

where the last term is integral of the $\mu(\alpha,\beta)$ function over the rectangular formed by two points: (α,β) and $(H_s,-H_s)$ for the diagonal corners.

If the $\mu(\alpha,\beta)$ function for real magnetic material is known, it is then possible to determine its complete magnetic characteristic – major and minor loops. Conversely, for any given (measured) magnetic characteristic with hysteresis, the corresponding $\mu(\alpha,\beta)$ function can be determined. Using the latter approach the weight function can be obtained from the differentiation of equation (5)

$$\mu(\alpha,\beta) = -\frac{\partial^2 T(\alpha,\beta)}{\partial\alpha\partial\beta} \quad (11)$$

Numerical implementation of (11) gives two main difficulties. First, differentiation of (5) can generate additional errors especially if significant errors are presented in $T(\alpha,\beta)$ measurements. Second, numerical evaluation of double integrals is usually time consuming procedure.

To model the hysteresis behavior the Preisach distribution function or the Everett function are needed. Several methods have developed to identify these functions. Some of the representative methods are described in [11-23].

Determination of the $T(\alpha,\beta)$ is generally based on measurement of a set of first order transition (reversal) curves [12], but for hard magnetic materials a set of minor symmetric loops is rather proposed [22]. These methods operate on the set of minor loops hence the relatively large amount of data are utilized. The $\mu(\alpha,\beta)$ can then be calculated by differentiating twice the $T(\alpha,\beta)$ according to (11). In order to avoid significant errors generated by numerical differentiating process a correction of the measured data is proposed [18].

Assuming the symmetry of the Preisach diagram about the α=-β line the factorisation property $\mu(\alpha,\beta)=\varphi(\alpha)\varphi(-\beta)$ can be used to identify the Preisach model as described in [11,13,14,20,21]. In this approach a $\varphi(\alpha)$ function is obtained from the major (usually limiting) hysteresis loop. Single valued $\varphi(\alpha)$ function is next approximated by analytical functions. Analytical solutions give relatively fast computation of the Preisach distribution function. To reduce calculation time the two dimensional wavelet average-interpolation technique is also proposed [23].

For some of the magnetic materials the $\mu(\alpha,\beta)$ can be analytically described by the Gauss distribution function [16,17] and a combination of Gauss and Lorentz distribution functions [19]. Representation of $\mu(\alpha,\beta)$ as a partial sum of functional series is also proposed [15].

In this paper the numerical implementation of the Preisach method is based on the limiting downward and upward loops.

3. THE IDENTIFICATION METHOD

3.1. Numerical implementation of the Preisach model

According to the chosen method, the weight function can be represented as the product of two single variable functions

$$\mu(\alpha,\beta)=\mu_a(\alpha)\mu_b(\beta) \tag{12}$$

Assuming the symmetry conditions about the α=-β line the following equation must be performed

$$\mu(\alpha,\beta)=\mu(-\beta,-\alpha) \tag{13}$$

From the (12) and (13) the following relations can be written:

$$\begin{aligned}&\mu_a(\alpha)\mu_b(\beta)=\mu_a(-\beta)\mu_b(-\alpha)\\&\mu_a(\alpha)=\mu_b(-\alpha)\\&\mu_b(\beta)=\mu_a(-\beta)\end{aligned} \tag{14}$$

Substituting the above in (10) yields

$$\begin{aligned}T(\alpha,\beta)&=\frac{B_u(\alpha)-B_d(\beta)}{2}+\int_{-H_s}^{\beta}\mu_b(\beta')d\beta'\int_{\alpha}^{H_s}\mu_a(\alpha')d\alpha'\\&=\frac{B_u(\alpha)-B_d(\beta)}{2}+F(-\beta)F(\alpha)\end{aligned} \tag{15}$$

where

$$F(\alpha)=\int_{\alpha}^{H_s}\mu_a(\alpha')d\alpha';\quad F(-\beta)=\int_{-H_s}^{\beta}\mu_a(-\beta')d\beta' \tag{16}$$

are functions which can be determined from measurements.

Applying equations (15) and (16) into (4), (6), and (7) the flux densities: $B_i(H)$, $B_u(H)$, and $B_d(H)$ can be expressed in terms of $F(H)$ and $F(-H)$ as follows:

$$B_i(H)=\frac{1}{2}\left[F(-H)-F(H)\right]^2 \tag{17}$$

$$B_u(H)=B_i(H)-F(H)^2 \tag{18}$$

$$B_d(H)=B_u(H)+2F(-H)F(H) \tag{19}$$

From the above equations the $F(H)$ function can be evaluated as

$$F(H)=\sqrt{\sqrt{\frac{B_d^2(H)+B_u^2(H)}{2}}-\frac{B_d(H)+B_u(H)}{2}},\quad H\geq 0 \tag{20}$$

$$F(H)=\sqrt{\sqrt{\frac{B_d^2(H)+B_u^2(H)}{2}}+\frac{B_d(H)+B_u(H)}{2}},\quad H<0 \tag{21}$$

3.2. Analytical interpolation of the Preisach model

The B_d and B_u values are measured at the nodes $H_i\in\{H_{-N},H_{-N+1},...,H_{-1},H_0,H_1,..H_N\}$. From this $2N+1$ samples of $F(H_i)$ are calculated. Next in each interval $[H_i, H_{i+1}]$ the $F(H_i)$ is interpolated by the cubic polynomial. Assuming continuity of the polynomial and of its first and second derivatives, at the node points the cubic spline piecewise interpolation of $F(H_i)$ is obtained. Thus the Everett function (15) is given as analytical formula. Finally, the Preisach distribution function (12) can be easily calculated.

4. EXPERIMENTAL VERIFICATION

4.1. Experimental setup

Measurements were carried out on grain oriented silicon steel strip of ET114-27 type. An iron core was prepared as tape wound torus. Its internal diameter is 506 mm and the cross section dimensions are 35 x 100 mm. The experimental setup is illustrated in Fig.8.

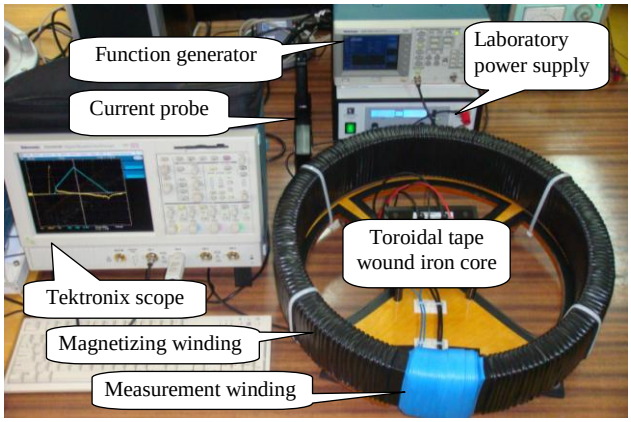

Fig.8. Experimental setup for measurement of hysteresis loops

The magnetizing winding is uniformly distributed on most of the core whereas the measurement winding is lumped on a small part of the torus. The magnetizing winding is energized by laboratory power supply PS 8000 DT type (*Elektro-Automatik GmbH*) controlled by function generator AFG3011 type (*Tektronix, Inc.*). The magnetic field is calculated from the current in the magnetizing coil, which is measured by means of TCP312 type current probe. The flux density is obtained by numerical integration of the voltage induced in the measurement coil. The core was

demagnetized before measurements. Measurements have been done under slow time varying excitation current. The current frequency equal to 0.020 Hz for the major loop was applied in other to reduce the dynamic effects in magnetic material.

4.1. Experimental results

The measured major hysteresis loop of tested core is shown in Fig.9. This is not a strict limited loop because material is not yet magnetically saturated. The relative magnetic permeability is μ_r=25 at H=2000 A/m. Nevertheless this loop is assumed as limited and used for further calculations of the $F(H)$ function which is shown in Fig.10 for the limiting range of field intensity.

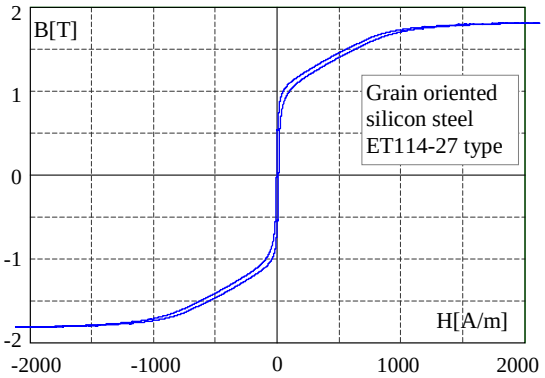

Fig.9. Measured *B-H* major hysteresis loop of tested material

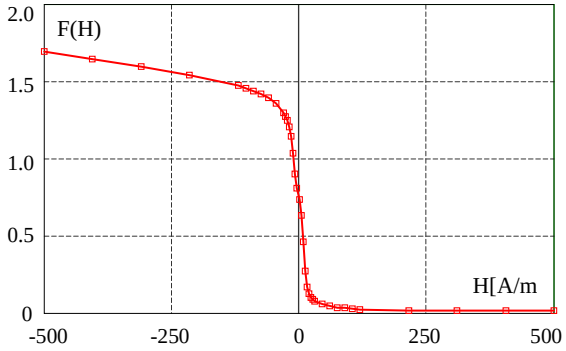

Fig.10. Calculated $F(H)$ function from major hysteresis loop

4.2. Representation of magnetic material

In this section the ability of the model to predict symmetric minor loops is examined. Some simulated and measured results of minor loops at different amplitudes of the field intensity H are shown in Fig.11 (H_{max}=44.4 A/m) and Fig.12 (H_{max}=110 A/m). It can be seen that the general agreement between both calculated and experimental results is satisfactory but there are small differences especially for relatively low values of H. The more accurate prediction needs to use modified Preisach models which will be presented in future work.

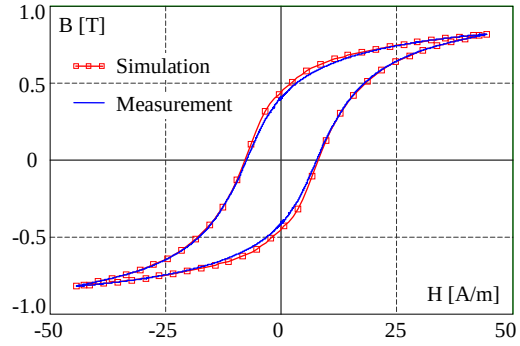

Fig.11. Simulated and measured symmetrical minor hysteresis loops – verification of applied model

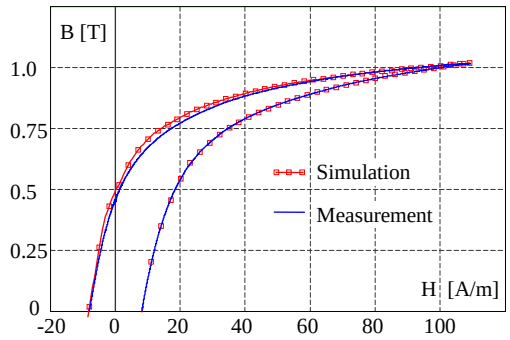

Fig.12. Simulated and measured symmetrical minor hysteresis loops – verification of applied model

The Everettt function of tested material is shown in Fig.13. The corresponding Preisach distribution function for the limiting range of the H is shown in Fig.14.

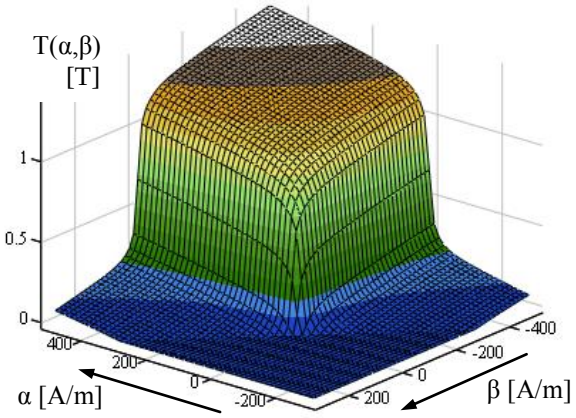

Fig.13. Everett function of grain oriented steel ET114-27 type

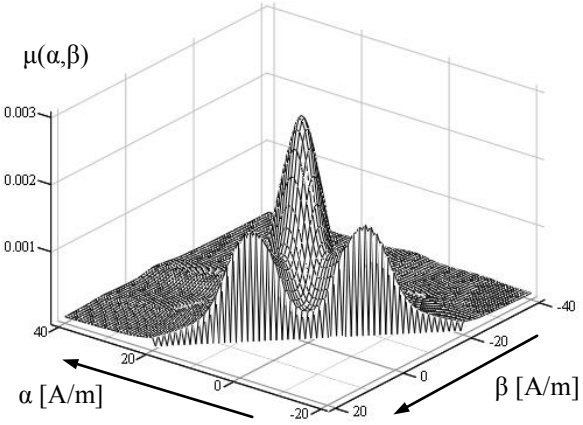

Fig.14. Preisach distribution function of the tested material

5. CONCLUSIONS

In this section the ability of the classical scalar Preisach model to predict magnetic behavior of the grain oriented silicon steel ET114-27 type was examined. The numerical implementation of the applied model is based on the factorisation property $\mu(\alpha,\beta)=\mu_a(\alpha)\mu_b(-\beta)$ of the Preisach distribution function. From this assumption the Everett function involves only the major hysteresis loop and product of $F(\alpha)$ and $F(-\beta)$ functions which are obtained from measurements and interpolated by the cubic polynomial splines.

The measured characteristic parameters of the major loop are: the saturation induction B_s=1.815 T, the saturation field H_s=2100 A/m, the remanence induction B_r=0.55 T, and the coercive field H_c=9 A/m. A good agreement is observed between the measured and simulated hysteresis loops. To increase the accuracy the modified Preisach models are needed.

6. REFERENCES

1. Germay N., Mastero S., Vroman J.: Review of ferroresonance phenomena in high-voltage power systems and presentation of a voltage transformer model for predetermining them, CIGRE, Paris, 1974, paper 33-18.
2. Teape J.W, Slater R.D., Simpson R.R.S., Wood W.S.: Hysteresis effects in transformers, including ferroresonance, Proc. IEE, Vol. 123, No. 2, 1976, pp. 153-158.
3. Talukdar S.N. Bailey J.R.: Hysteresis models for systems studies, IEEE Transactions on Power Apparatus and Systems, Vol. PAS-95, no. 4, 1976, pp. 1429-1434.
4. Preisach F.: Über die magnetische Nachwirkung, Zeitschrift für Physik, Bd.94, 1935, pp. 274-302.
5. Krasnosel'skii, M.A. and Pokrovskii, A.V.: Sistemy s gisterezisom (Systems with Hysteresis), Moskow: Nauka, 1983.
6. Mayergoyz I. D.: Mathematical models of hysteresis, IEEE Transactions on Magnetics, Vol. MAG-22, No.5, Sept. 1986, pp.603-608.
7. Mayergoyz I.D., Friedman G.: Generalized Preisach model of hysteresis, IEEE Transactions on Magnetics, Vol.24, No.1, Jan.1988, pp. 212-217.
8. Mayergoyz I.D.: Dynamic Preisach models of hysteresis, IEEE Transactions on Magnetics, Vol.24. No.6, Nov. 1988, pp. 2925-2927.
9. Iványi A., Füzi J., Szabó Z.: Preisach models of ferromagnetic hysteresis, Przegląd Elektrotechniczny, R. LXXIX 3/2003, s.145-150.
10. Everett D.: A general approach to hysteresis – Part 4., An alternative formulations of the domain model, Trans. Faraday Society, vol.51, 1955, pp. 1551-1557.
11. Hui S.Y.R., Zhu J.: Numerical modeling and simulation of hysteresis effects in magnetic cores using transmission-line modeling and the Preisach theory, IEE Proc. -Electr. Power App, Vol. 142, No.1, Jan. 1995, pp. 57-62.
12. Mayergoyz I.D.: On numerical implementation of hysteresis models, IEEE Transactions on Magnetics, Vol. Mag-21, No.5, Sept. 1985, pp. 1853-1855.
13. Naidu S.R.: Simulation of hysteresis phenomenon using Preisach's theory, IEE Proceedings, Vol.137, Pt. A. No. 2, March 1990, pp.73-79.
14. Prousalidis J.M., Hatziargyriou N.D., Papadias B.C.: Representation of hysteresis in three-phase transformer models for electromagnetic transients, IEE Proc.-Electr. Power Appl., Vol. 143, No. 4, July 1996, pp. 331-338.
15. Coulson M.A., Slater R.D., Simpson R.R.S.: Representation of magnetic characteristic, including hysteresis, using Preisach's theory, Proc. IEE, Vol. 124, No. 10, Oct. 1997, pp. 895-898.
16. Debruyne H., Clenet S., Piriou F.: Characterisation and modeling of hysteresis phenomenon, Mathematics and Computers in Simulation, 46, 1998, pp. 301-311.
17. Hong S.K., Kim H.K., Jung H.K.: Formulation of the Everett function using least square method, IEEE Transactions on Magnetics, Vol.34, No.5, Sept. 1998, pp. 3052-3055.
18. Wulf M., Vandevelde L., Maes J., Dupre L., Melkebek J.: Computation of the Preisach distribution function based on a measured Everett map, IEEE Transactions on Magnetics, Vol.36, No.5, Sept. 2000, pp. 3141-3143.
19. Füzi J.: Analythical approximation of Preisach distribution functions, IEEE Transactions on Magnetics, Vol.39, No.3, May 2003, pp. 1357-1360.
20. Ragusa C.: An analythical method for the identification of the Preisach distribution function, Journal of Magnetism and Magnetic Materiale 354-255, 2003, pp. 259-261.
21. Szabó Z., Tugyi I., Kádár G., Füzi J.: Identification procedures for scalar Preisach model, Physica B 343, 2004, pp. 142-147.
22. Dlala E., Saitz., Arkkio A.: Hysteresis modeling based on symmetric minor loops, IDEE Trans. on Magnetics, Vol.41, No.8, Aug 2005, pp. 2343-2348.
23. Schiffer A., Iványi A.: Preisach distribution function approximation with wavelet interpolation technique, Physica B 372, 2006, pp. 101-105.

WYKORZYSTANIE TEORII PREISACHA DO MODELOWANIE HISTEREZY MAGNETYCZNEJ RDZENIA ZWIJANEGO Z TAŚMY

Słowa kluczowe: Histereza magnetyczna, Teoria Preisacha, Funkcja Everetta, Funkcja dystrybucji Preisacha.

W referacie przedstawiono model matematyczny histerezy magnetycznej w ujęciu klasycznej teorii Preisacha. Dokonano implementacji skalarnego modelu Preisacha w odniesieniu do rdzenia zwijanego z taśmy typu ET114-27. Do symulacji różnych stanów magnetycznych rdzenia wykorzystano jedynie dane z pomiarów głównej pętli histerezy. Wyznaczono funkcję Everetta i funkcję dystrybucji Preisacha badanego rdzenia. Uzyskano ogólnie dobrą zgodność wyników symulacji z wynikami pomiarów.